Interfacial activity and contact angle of homogeneous, functionalized and Janus nanoparticles at the water/decane interface

Miguel Angel Fernandez-Rodriguez,[†] Jose Ramos,[‡] Lucio Isa,[¶] Miguel Angel Rodriguez-Valverde,[†] Miguel Angel Cabrerizo-Vilchez,[†] and Roque Hidalgo-Alvarez[*,†]

Biocolloid and Fluid Physics Group, Applied Physics Department, Faculty of Sciences, University of Granada, Granada, Spain, POLYMAT, Bionanoparticles Group, Applied Chemistry Department, UFI 11/56, Faculty of Chemical Sciences, University of País Vasco UPV/EHU Donostia-San Sebastián, Spain

Department of Materials, Department of Bioengineering, and the Institute for Biomedical Engineering, Imperial College London, London SW7 2AZ, United Kingdom, and Laboratory for Interfaces, Soft matter and Assembly, ETH Zürich, Vladimir-Prelog-Weg 5, 8093 Zürich, Switzerland

E-mail: rhidalgo@ugr.es

[*]To whom correspondence should be addressed

[†]Biocolloid and Fluid Physics Group, Applied Physics Department, Faculty of Sciences, University of Granada, Granada, Spain

[‡]POLYMAT, Bionanoparticles Group, Applied Chemistry Department, UFI 11/56, Faculty of Chemical Sciences, University of País Vasco UPV/EHU Donostia-San Sebastián, Spain
Department of Materials, Department of Bioengineering, and the Institute for Biomedical Engineering, Imperial College London, London SW7 2AZ, United Kingdom

[¶]Laboratory for Interfaces, Soft matter and Assembly, ETH Zürich, Vladimir-Prelog-Weg 5, 8093 Zürich, Switzerland

Abstract

Surface heterogeneity affects the behavior of nanoparticles at liquid interfaces. To gain deeper understanding on the details of these phenomena, we have measured the interfacial activity and contact angle at water/decane interfaces for three different types of nanoparticles: homogeneous PMMA, silica functionalized with a capping ligand and containing a methacrylate terminal group and Ag-based Janus colloids with two capping ligands of different hydrophobicity. The interfacial activity was analyzed by pendant drop tensiometry and the contact angle was measured directly by Freeze-fracture Shadow-Casting cryo-SEM. The silver Janus nanoparticles presented the highest interfacial activity, while the silica nanoparticles showed higher interfacial activity and contact angle compared to the homogeneous PMMA nanoparticles. Additionally, increasing the bulk concentration of the PMMA and silica nanoparticles up to 100-fold compared to the Janus nanoparticles, led to silica particles forming fractal-like structures at the interface, contrary to the PMMA particles that did not show any spontaneous adsorption.

Keywords: Interfacial activity; FreSCA cryo-SEM; Pendant drop tensiometry; Janus nanoparticles; Water/decane interface.

Introduction

Janus particles with two spatially separated domains displaying different physicochemical properties are suitable to develop responsive nanomaterials.[1,2] The physicochemical differences between the domains of such nanoparticles enable their self-assembly or reorientation as a response to a given stimulus (e.g., changes in the pH, temperature, ionic strength, ...)[2].

In particular, Janus particles obtained from the partial surface modification of silica particles via silane functionalization have been successfully validated for different applications, such as catalysis,[3] ultrahydrophobic films,[4] water-repellent fabrics[5] and as emulsion[6–8] and foam[9] stabilizers.

The usual way to synthesize Janus nanoparticles involves the selective functionalization of each hemisphere with different capping ligands.[1] A different approach has been reported for heterogeneous silver nanoparticles functionalized with two capping ligands with different hydrophobicity.[10] The capping ligands on such silver nanoparticles reorient towards the preferred liquid phase when placed at a water/oil interface, becoming Janus nanoparticles in situ.[10,11]

Although they are used as interfacial stabilizers, the behavior of Janus particles at liquid interfaces is still controversial.[9,12] The measured contact angle of nanoparticles at interfaces depends on the technique used.[12] In particular, the hydrophobicity of silica nanoparticles is affected by the addition of surface-active molecules such as surfactants or alcohols.[13] Thus, the effect of the spreading agent in Langmuir isotherm experiments must be taken into account because it can affect the final surface tension and the contact angle of the deposited particles.[11,12]

The problem of measuring contact angles of Janus particles is even more complex. Whether Janus particles actually behave as amphiphiles at the interface or not depends on the Janus ratio (i.e. the ratio between the areas of the two different domains) and the wettability contrast between both patches. Strictly real Janus behavior, namely the correspondence of the three-phase contact line with the boundary between domains, can only be observed for Janus ratios close to unity and large wettability contrasts. How this scenario demonstrated for microparticles is applicable to nanoparticles is still a matter of debate.[14]

Regardless of all the controversy, Janus nanoparticles act as better emulsion stabilizers than homogeneous nanoparticles. It is known that Janus nanoparticles obtained by surface modification of bare silica particles successfully allow to stabilize oil droplets in water with higher long-term stability than emulsions stabilized with homogeneous silica nanoparticles.[15] This fact agrees with the theoretical prediction that a Janus particle with equal hydrophilic and hydrophobic areas is three times more surface active than the corresponding homogeneous particles at a water/oil interface.[16] Moreover, in the case of nanoparticles, the thickness of the capping ligands is usually comparable to the core size. Therefore, ligand reconfiguration can affect the adsorption of the nanoparticles at liquid interfaces, as shown by molecular dynamic simulations and experiments[9] and complicated energies and interactions within the polymer capped nanoparticles govern the formation of nanostructures.[17]

In this work, we focused on the comparison between contact angle and interfacial activity of three different nanoparticles at the water/decane interface: polymethylmethacrylate homogeneous nanoparticles, silica nanoparticles functionalized with methacryloxypropyltrimethoxysilane and silver Janus nanoparticles. We measured the contact angle of these nanoparticles with Freeze-fracture Shadow-casting cryo-SEM[14,18] and the interfacial tension with a pendant drop tensiometer.

Materials and Methods

Homogeneous, functionalized and Janus nanoparticles

Polymethylmethacrylate (PMMA) Research Particles of radius 105 nm, SD=4 nm, 5% w/v aqueous suspension (Microparticles GmbH, Germany) were used as homogeneous nanoparticles (labeled as PMMA-HPs).

Tetraethyl orthosilicate (TEOS, Acros Organics, 98%), ethanol (Scharlau, absolute, reagent grade), ammonia (Scharlau, solution 32%), methacryloxypropyltrimethoxysilane (MPS, Sigma-Aldrich) and ultrapure distilled water (Milli-Q Academic, Millipore) were used for the synthesis of silica nanoparticles according to the Stöber procedure.[19] For each reaction, absolute ethanol, ammonia, and water were mixed in a 500 mL reaction vessel. Then TEOS was added quickly and the reaction mixture was stirred at 350 rpm and room temperature for 24h. The molar concentration of the mixed solution was water/ammonia=2.49/1.06 for the synthesis of silica nanoparticles of 208 nm in diameter. The volume of absolute ethanol was adjusted up to 500 mL and the concentration of TEOS was fixed to 0.2 M. Silica nanoparticles were collected by centrifugation (15000 rpm, 15 $min.$) and washed by repeated redispersion in absolute ethanol three times. The final product was dried in a vacuum oven at 80 °C for 24h. The method of partial functionalization of silica nanoparticles was reported in previous works.[20–22] First, 1.6 g of silica nanoparticles were introduced into a beaker. Next, 0.8 mL deionized water were added to the silica nanoparticles. Then, 52 mL of toluene containing 1.0 mL of MPS and 2.0 mL of triethylamine were added. The mixture was stirred for 3 days at room temperature. Subsequently, the solid was collected by centrifugation (12000 rpm, 5 $min.$), and dried under vacuum for 24 h after being washed three times in ethanol.

These silica nanoparticles are partially modified with MPS because a fraction of the particle surface remains covered with hydroxyl groups with high affinity to water, and the other fraction of the particle surface is modified with MPS groups, less polar and with higher affinity to oil. From thermogravimetric analysis, assuming that the amount of MPS is homogeneously distributed over all the surface, the MPS surface coverage is $2.27 \cdot 10^{-4}\, mol_{MPS}/g_{SiO_2}$. The final silica functionalized nanoparticles are labeled as silica-FPs and are dispersed in MilliQ water.

Silver Janus nanoparticles (labeled as Ag-JPs) were synthesized as described in previous work [11] with a size of $175\, nm$ measured by SEM. The synthesis is based in the exchange of 11-mercaptoundecanoic acid and 1-undecanthiol ligands with silver nanoparticles functionalized with decanoic acid. The Ag-JPs are dispersed in methanol.

All nanoparticle dispersions are surfactant free. The size and electrophoretic mobility of the nanoparticles were measured by Dynamic Light Scattering with a Malvern Zetasizer Nano Z device in a solution of BrK at an ionic strength of $10^{-4}\, M$ and a pH of 5.5.

Pendant drop tensiometry

Pendant drop tensiometry was performed with a homemade setup as described in previous works. [11,23] First, a water pendant drop was formed in a capillary with a Hamilton microinjector pump. Different amounts of Ag-JPs dispersed in methanol were deposited with a Hamilton microsyringe on the surface of the initial water pendant drop. In the case of PMMA-HPs and silica-FPs, the microsyringe was loaded with a 1:1 particle dispersion/methanol mixture. Once the pendant drop was formed, side-view images of the droplet were captured by a CMOS camera and processed with the Dinaten software to obtain the corresponding surface tension by Axisymmetric Drop Shape Analysis of the pendant drop profile (ADSA-P). [24] The surface tension was monitored until full evaporation of the methanol (i.e. Langmuir layer formation [9]). Next, we immersed the pendant drop in decane (HPLC grade, Sigma) and performed growing and shrinking cycles at $0.08\, \mu L/s$, varying the drop volume within $40\, \mu L$ and $15\, \mu L$ as described in previous works, [11,23] and the corresponding interfacial tension was measured. In addition, drops of the suspensions containing the nanoparticles at different concentrations were formed in the case of aqueous suspensions (PMMA-HPs and silica-FPs). In this process the particles adsorb at the interface from the pendant drop

bulk (i.e. Gibss layer formation, significantly slower than the Langmuir layer formation [9]).

Freeze-fracture Shadow-Casting

The Freeze-fracture Shadow-Casting (FreSCa) cryo-SEM technique, described in previous works, [14,18] consists of the immobilization and imaging of nanoparticles at a water/oil interface in a cryo-SEM. The immobilization is provided by vitrification of the interface with a propane jet freezer and the imaging is performed after fracturing the sample in cryo and ultra-high vacuum conditions and after directional coating by a thin tungsten layer, deposited at a 30° angle relative to the interface. The shadow projected by the nanoparticles trapped in the water/decane interface upon tungsten casting is measured by cryo-SEM and used to calculate the contact angles of individual nanoparticles. The silica-FPs and PMMA-HPs are measured forming the water phase directly with the water particle suspension and the Ag-JPs are deposited from methanol in a water phase and we wait until full evaporation of the methanol. Thus, the methanol evaporation process is absent for silica-FPs and PMMA-HPs and we expect lower number of nanoparticles reaching the interface because of the absence of the energy provided by the methanol evaporation.

Results and Discussion

The results of electrophoretic mobility, size and contact angle measured for the different nanoparticles are collected in Table 1. First, we discuss the similarities and differences between nanoparticles to establish possible comparisons. The capping ligands of the silica-FPs consist in a silane group anchored to the silica core, a propyl hydrocarbon chain and a terminal methacrylate group. The silica-FPs are comparable in size and mobility with the PMMA-HPs, both dispersed in water. The PMMA-HPs nanoparticles serve as an example of homogeneous organic nanoparticle and the silica-FPs as a heterogeneous nanoparticle made of a silica inorganic core (hydrophilic) and less hydrophilic organic capping ligands. On the other hand, the Ag-JPs are also comparable in size with the other nanoparticles, but their mobility is lower (half) and they are dispersed in methanol. Moreover, the capping ligands of the Ag-JPs are reoriented at the water/oil interface into different spatial domains, with the more hydrophilic one towards the water phase and the more hydrophobic

one towards the oil phase.[10,11] When the capping ligands do not present a difference in hydrophobicity, simulations have shown that the Janus particles place randomly at the interface although there is some ordering when the interface is stretched.[25]

From Table 1, the nanoparticle size is systematically overestimated by DLS compared to the direct measurement obtained from the FreSCa cryo-SEM images (see Figure 2). This is expected because DLS gives an effective hydrodynamic radius that is greater than the real radius of the dehydrated nanoparticles.

The contact angle distribution was measured counting 176 PMMA-HPs, 229 silica-FPs and 53 Ag-JPs. The lower number of Ag-JPs is due to the lower concentration that we could obtain with these nanoparticles. The values of contact angle in Table 1 were calculated as the mean and standard deviation of the measured contact angles for each kind of nanoparticle. The contact angles obtained with the FreSCa cryo-SEM technique for the silica-FPs, PMMA-HPs and Ag-JPs deposited at water/decane interfaces present a wide distribution (see Figure 1). Nevertheless, the distribution is narrower for the PMMA-HPs than for the silica-FPs and Ag-JPs. The silica-FPs presented the highest contact angle (over 90°). Followed by the Ag-JPs (close to 90°), and finally the PMMA-HPs (76°). The values of contact angle enable to predict the behavior of the nanoparticles as emulsifiers: contact angles smaller than 90° tend to stabilize oil-in-water emulsions and values greater than 90° tend to stabilize water-in-oil emulsions.[26] Nonetheless, this emulsion stabilization mechanism has to be taken carefully into consideration because it is affected by coalescence effects. Stancik et al.[27] studied the coalescence of particle-laden drops with homogeneous particles and found that the precise nature of the particle dynamics and microstructures during coalescence are not straightforward to anticipate.

The wide distribution of measured contact angles agrees with the results obtained with other techniques for direct contact angle measurement of nanoparticles placed at liquid interfaces such as Gel Trapping Technique[28] or Bessel Beam Microscopy.[29] We assume that this scattering is due to the dependence of the contact angle on the details of the different nanoparticles and on their kinetics as they reach the interface. Furthermore, the narrower distribution of contact angles for the PMMA-HPs might point out to less contact angle variation of the homogeneous nanoparticles rather than the heterogeneous nanoparticles. The high contact angle of the silica-FPs, compared to

PMMA-HPs, is in agreement with previous molecular dynamics simulations of silica nanoparticles (3 nm-diameter) with tunable surface activity at a water/decane interface.[26] In this work, the surface activity was modulated through the ratio between methyl and hydroxyl groups at the interface and the homogeneous nanoparticles presented contact angles typically lower than 90°, whereas the Janus nanoparticles revealed contact angles usually greater than 90°. Even although our silica-FPs are not strictly Janus nanoparticles, they are less hydrophilic than the homogeneous PMMA nanoparticles. The macroscopic contact angle of a water drop deposited on a smooth PMMA film was reported to be $(67.8 \pm 1.4)^\circ$ (water/air interface), although with a later treatment that provided more roughness and functional groups reorientation to the PMMA film, the contact angle increased up to $(154.3 \pm 3.9)^\circ$.[30] The contact angle of PMMA-HPs of the same manufacturer but with a larger size $(1 - 2\,\mu m)$ measured by Gel Trapping Technique in a water/n-octane interface was $(56 \pm 2)^\circ$,[31] which is significantly lower than the value obtained for our PMMA-HPs at a water/decane interface measured by FreSCa cryo-SEM. This reveals a strong dependence of the observed contact angle and specific PMMA surface, i.e. in terms of the particle size, roughness and in relation to the type of oil phase. This invalidates any comparison between the contact angle of a sessile water drop on a PMMA substrate and the contact angle of PMMA-HPs deposited at a water/oil interface. Finally, the Ag-JPs contact angle seems lower than the one of the silica-FPs but actually they overlap within their standard deviations. From this, we cannot state differences between these nanoparticles.

Table 1: Electrophoretic mobility and size measured by Dynamic Light Scattering (DLS) and size and contact angle (CA) measured by FreSCa cryo-SEM of the nanoparticles studied:

	Mobility $(10^{-8}\, m^2/(V \cdot s))$	DLS size (nm)	FreSCa size (nm)	FreSCa CA $(^\circ)$
PMMA-HPs	-2.7 ± 0.6	156.9 ± 0.5	119 ± 27	76 ± 9
Silica-FPs	-3.0 ± 0.4	216 ± 16	181 ± 23	94 ± 14
Ag-JPs	-1.5 ± 0.6	210 ± 18	175 ± 43	86 ± 19

In order to investigate further the effects of surface chemistry on the behavior at the interface, the interfacial activity of the nanoparticles was explored by pendant drop tensiometry. Stable interfacial tension values were obtained after forming water pendant drops with different number of particles deposited in air and subsequently immersed in decane. The numbers of particles were

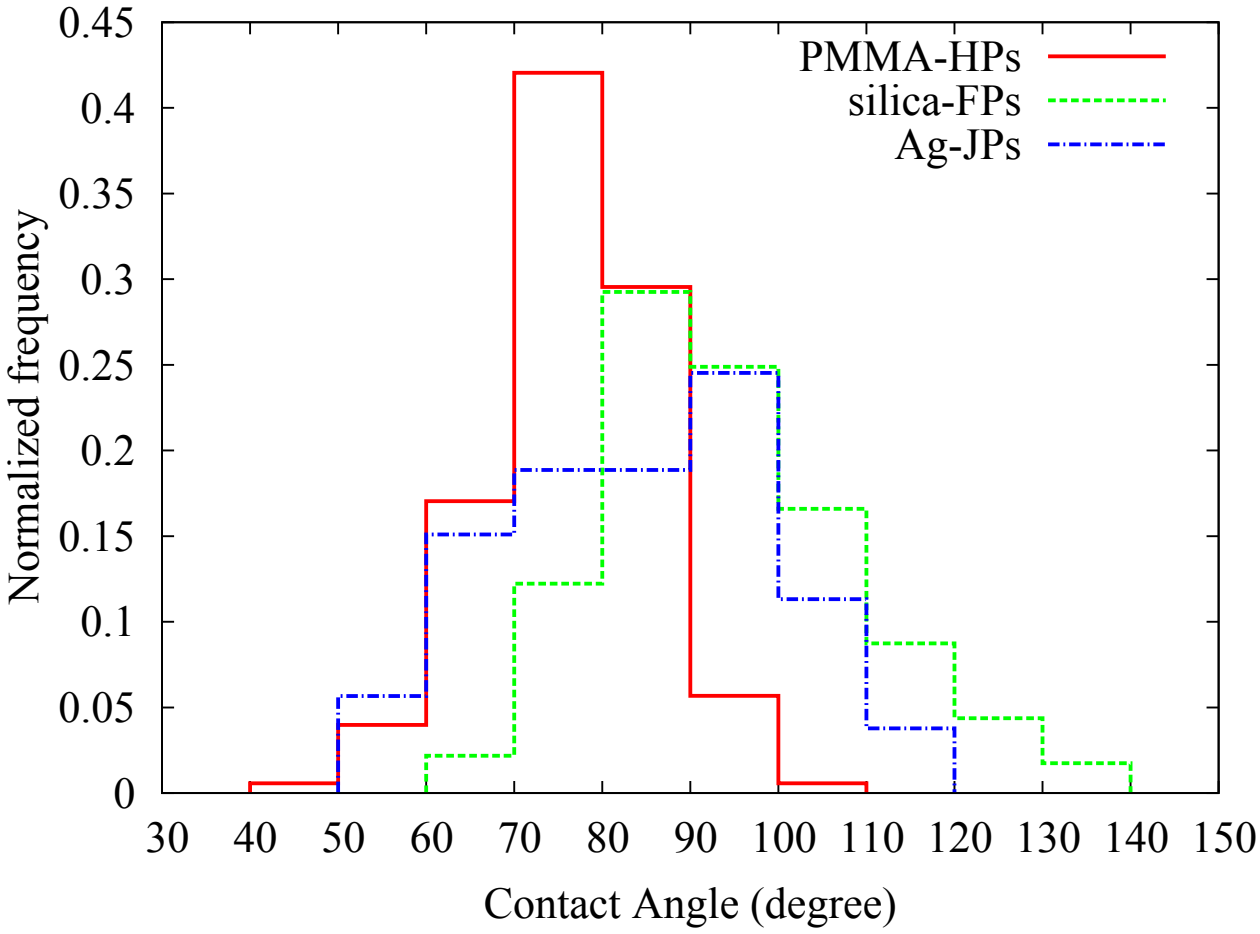

Figure 1: Contact angle of PMMA homogeneous nanoparticles (PMMA-HPs), silica functionalized nanoparticles (silica-FPs), and silver Janus nanoparticles (Ag-JPs) at water/decane interfaces measured by FreSCa cryo-SEM.

chosen to get the same coverage between different nanoparticles starting from the assumption that all of them were placed at the interface assuming close-packing. The stable values of interfacial tension are collected in Table 2, measured after 30 min.

Table 2: Interfacial tension of a $20\,\mu L$ water pendant drop in air and of a $30\,\mu L$ water pendant drop in decane, for different concentrations of each nanoparticle upon spreading.

	$\gamma_{\text{Water/Air}}\,(mN/m)$	$\gamma_{\text{Water/Decane}}\,(mN/m)$
$2.43 \cdot 10^8$ PMMA-HPs	72.7 ± 0.1	50.2 ± 0.2
$4.86 \cdot 10^8$ PMMA-HPs	70.5 ± 0.1	52.2 ± 0.1
$9.72 \cdot 10^8$ PMMA-HPs	72.4 ± 0.1	52.3 ± 0.1
$1.05 \cdot 10^8$ silica-FPs	70.3 ± 0.1	52.2 ± 0.1
$2.10 \cdot 10^8$ silica-FPs	71.4 ± 0.1	50.3 ± 0.1
$4.20 \cdot 10^8$ silica-FPs	70.0 ± 0.1	51.1 ± 0.1
$0.96 \cdot 10^8$ Ag-JPs	71.8 ± 0.2	48.3 ± 0.5
$1.92 \cdot 10^8$ Ag-JPs	71.0 ± 0.4	48.5 ± 0.5
$3.84 \cdot 10^8$ Ag-JPs	64.1 ± 0.4	42.9 ± 0.4

At room temperature, the water surface tension is around 72 mN/m and the water/decane interfacial tension around 52 mN/m. The values in Table 2 confirm that the surface tension of the PMMA-HPs and silica-FPs suspensions do not depend on the particle concentration. Although the errors are low because the values are constant over time, within a 2 mN/m margin it is not possible to say that they differ significantly due to the limits of the pendant drop tensiometry. Only for the Ag-JPs at the highest concentration, the surface tension was significantly decreased. This might point out that the PMMA-HPs and silica-FPs are scarcely adsorbed at the water/air interface or that they are very low interfacial active. However, all nanoparticles certainly adsorbed at the water/decane interface as shown in Table 2 and Figure 2. Provided the extensive use of silica nanoparticles as emulsion stabilizers, these results point out that they stabilize through an steric effect rather than by its amphiphile character.[16]

The results of compression/expansion cycles of each water pendant drop immersed in decane are plotted in Figure 3 where the interfacial pressure Π is defined as $\Pi = \gamma_0 - \gamma$, with γ_0 the interfacial tension in absence of nanoparticles. The interfacial pressure is plotted against the normalized area. The normalized area is calculated as the pendant drop area divided by the total area that the nanoparticles would occupy if they were all placed at the interface, assuming close-packing. The piecewise-like compression isotherms are similar to the observed ones for other Janus systems

studied previously and they are piecewise-like due to the limitations to vary the interfacial area over a large range in a single pendant drop experiment.[11,23] When a film is compressed beyond a certain pressure (i.e. the pendant drop is shrunk) a particle-laden drop may undergo buckling.[32] When buckling occurs, it is expected to observe a change in the slope of the compression isotherm.[33] However, this behavior is not observed in our measurements and this suggests the absence of such buckling processes within the range of volumes and interfacial tensions studied. Also, the compression/expansion cycles in Figure 3 were closed for each concentration and nanoparticle, pointing out that there was no significant adsorption or desorption during the experiments. The silver-JPs showed discontinuities in the surface pressure for similar compression states. This might indicate that they are very sensitive to the initial compression state upon adsorption of different particle numbers. In fact, the monolayers may evolve differently when the surface is compressed and the internal stress may relax in different ways. Finally, it can be concluded that Ag-JPs presented significantly higher interfacial activity, compared to the negligible interfacial activity of silica-FPs and PMMA-HPs as previously demonstrated. In order to try and obtain a similar surface pressure as the Ag-JPs for the other two nanoparticle types, we performed different experiments in which the pendant drop was made of the aqueous silica-FPs and PMMA-HPs dispersions. In this case we did not spread the particles aided by methanol, but we monitored the spontaneous adsorption from the bulk. Under these conditions the available number of particles that can adsorb at the interface could be increased 100 times. The results of compression/expansion cycles of such water pendant drops immersed in decane are plotted in Supporting Information (see Fig. S1).

The PMMA-HPs and silica-FPs, similar in size and with the same particle number in the water bulk phase, behave differently at the water/decane pendant drop interface. Compared to the homogeneous aspect of the pendant drop of PMMA-HPs (Figure 4a), the silica-FPs are visibly accumulated with fractal-like structures at the bottom of the drop (Figure 4b). The number of particles that reach the interface will be different due to electrostatic repulsions and dipolar interactions through the oil phase and to the different and slow relaxation processes of such particles reaching the interface.[34] The fractal-like structure of silica-FPs is in agreement with a study in which silica nanoparticles form dense patches connected between them and surrounding uncovered areas.[7] Some authors report that the homogeneous nanoparticles are arranged in a hexagonal pattern

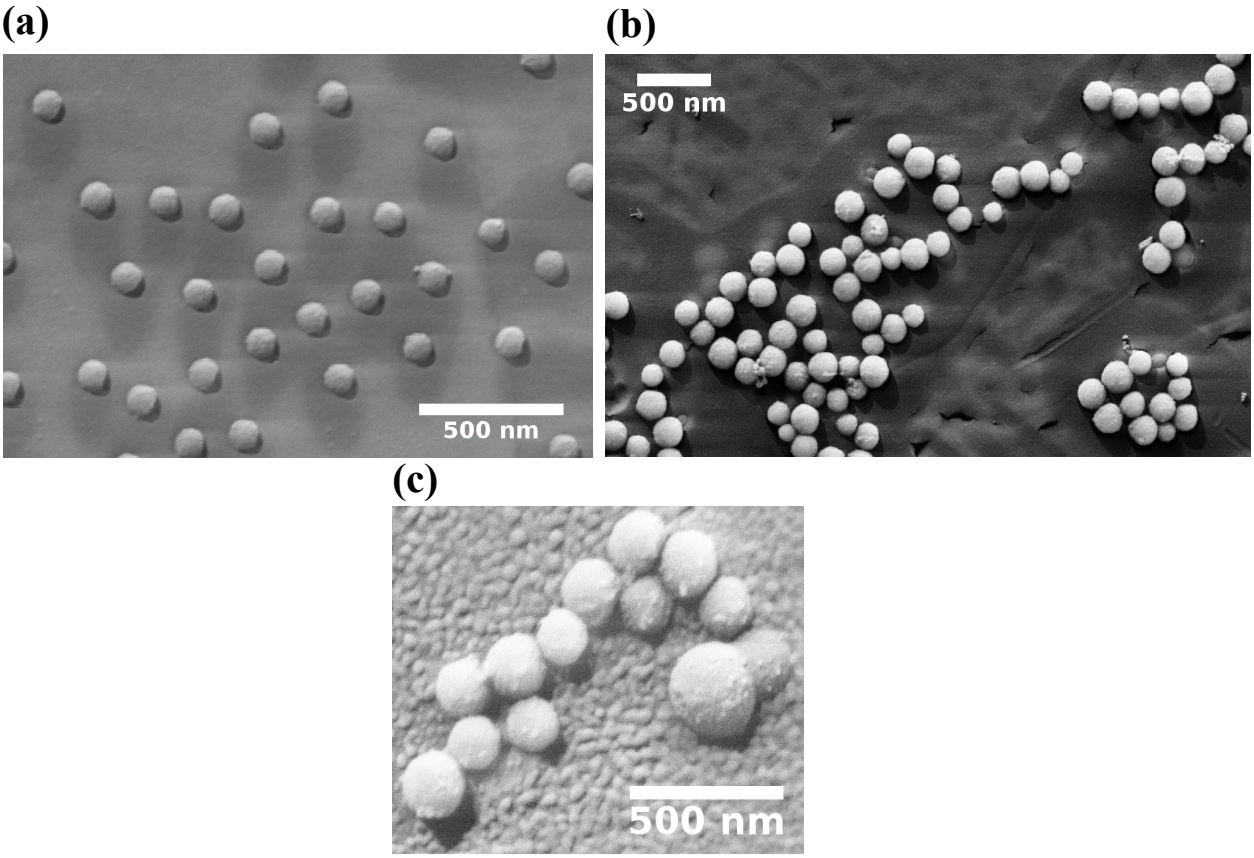

Figure 2: FreSCa cryo-SEM pictures of (a) PMMA-HPs, (b) silica-FPs and (c) Ag-JPs. The tungsten shadow projected by the nanoparticles enables estimating the contact angle of the nanoparticles. All the scale bars are $500\,nm$.

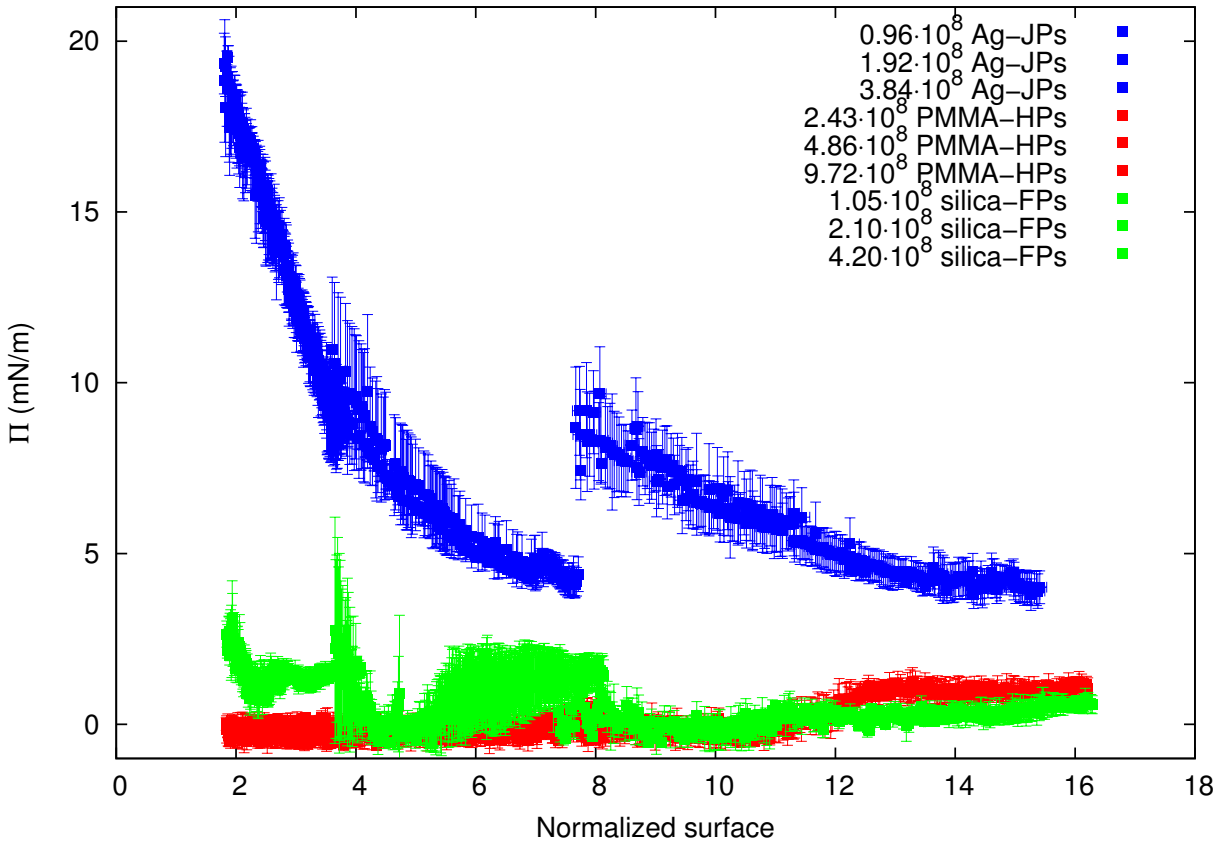

Figure 3: Interfacial pressure for compression/expansion cycles of water/decane pendant drops against the normalized area for different concentrations of deposited PMMA-HPs, silica-FPs and Ag-JPs. The normalized area is calculated as the pendant drop area divided by the area that would be occupied by the nanoparticles if they were all placed at the interface, assuming close-packing.

due to long-range electrostatic repulsion, contrary to Janus nanoparticles that show a fractal-like arrangement due to attractive interactions.[35,36] Furthermore, Xu et al.[37] observed attraction and repulsion of homogeneous particles in a water/oil pendant drop. This effect was observed when a water drop (immersed in an oil phase) was brought close to a flat oil-water interface due to electrostatic interactions between the two interfaces. The attractive interactions for silica-FPs might be due to capillary interactions, where different roughness or chemical heterogeneity may deform the three phase contact line around the particle, leading to nanoparticle aggregation.[38] Finally, the FreSCa images in Figure 2 also indicate that the silica-FPs have stronger tendency to aggregate at the interface compared to the PMMA-HPs.

(a) Homogeneous PMMA nanoparticles (b) Functionalized silica nanoparticles

Figure 4: $5\,\mu L$ pendant drops with a suspension of $21.7 \cdot 10^{11}$ nanoparticles per mL of (a) PMMA-HPs and (b) silica-FPs, both immersed in decane. The presence of fractal-like clusters of the silica-FPs is clearly noticeable in the images.

Conclusions

The interfacial activity of homogeneous PMMA nanoparticles (PMMA-HPs), functionalized silica nanoparticles (silica-FPs) and Janus silver nanoparticles (Ag-JPs) with similar sizes ($\sim 200\,nm$), was studied at the water/decane interface via interfacial tension and direct contact angle measurements. The highest contact angle was obtained for the silica-FPs and Ag-JPs and the lowest for the PMMA-HPs. The wide contact angle distribution for all nanoparticles might be due to the heterogeneity in the surface properties and adsorption of the nanoparticles that reach the interface. The interfacial activity of Ag-JPs was significantly higher, compared to silica-FPs and PMMA-HPs at equivalent particle concentrations. Although the silica-FPs and PMMA-HPs do not show a strong effect in reducing the water/decane interfacial tension, they were certainly adsorbed as reflected by FreSCA cryo-SEM images. A 100-fold higher concentration of silica-FPs and PMMA-HPs was necessary to obtain a similar reduction of the interfacial tension at the water/decane interface as for the case of the Ag-JPs. Thus, the silica nanoparticles are expected to stabilize emulsions by steric effect rather than by its amphiphile character. At higher concentrations, the silica-FPs exhibited fractal-like structures due to attractive interactions unlike PMMA-HPs. Despite the fact that the contact angles of silica-FPs and Ag-JPs were similar within errors, only the latter one led to a significant reduction of the interfacial tension at the same surface coverage probably due to its surface chemistry and Janus character. From our findings, in absence of surfactants, Janus silver nanoparticles may act as better emulsifiers due to their remarkable interfacial activity at the water/decane interface, compared with homogeneous PMMA or heterogeneously functionalized silica nanoparticles.

Acknowledgement

This work was supported by the Spanish MINECO (projects MAT2011-23339 and MAT2013-44429-R), by "Junta de Andalucía" and FEDER (projects P10-FQM-5977 and P12-FQM-1443) and by the COST Action "Smart and green interfaces" (STSM MP1106-14761). Lucio Isa acknowledges financial support from the Swiss National Science Foundation (grant PP00P2-144646/1). The authors thank Prof. Nicholas Spencer at ETH Zurich for the access to equipment and facilities

and J.A. Holgado-Terriza and J.L. Muros-Cobos for the software Dinaten© used for the interfacial tension measurements. The authors acknowledge support of ScopeM/Swiss Federal Institute of Technology ETHZ for the FreSCa cryo-SEM measurements.

References

(1) Walther, A.; Müller, A. H. E. Janus Particles: Synthesis, Self-Assembly, Physical Properties, and Applications. *Chem. Rev.* **2013**, *113*, 5194–5261.

(2) Yoshida, M.; Lahann, J. Smart Nanomaterials. *ACS Nano* **2008**, *2*, 1101–1107.

(3) Faria, J.; Ruiz, M. P.; Resasco, D. E. Phase-Selective Catalysis in Emulsions Stabilized by Janus Silica-Nanoparticles. *Adv. Synth. Catal.* **2010**, *352*, 2359–2364.

(4) Berger, S.; Ionov, L.; Synytska, A. Engineering of Ultra-Hydrophobic Functional Coatings Using Controlled Aggregation of Bicomponent Core/Shell Janus Particles. *Adv. Funct. Mater.* **2011**, *21*, 2338–2344.

(5) Synytska, A.; Khanum, R.; Ionov, L.; Cherif, C.; Bellmann, C. Water-Repellent Textile via Decorating Fibers with Amphiphilic Janus Particles. *ACS Appl. Mater. Interfaces* **2011**, *3*, 1216–1220.

(6) Binks, B. P.; Tyowua, A. T. Influence of the degree of fluorination on the behaviour of silica particles at air-oil surfaces. *Soft Matter* **2013**, *9*, 834–845.

(7) Destribats, M.; Gineste, S.; Laurichesse, E.; Tanner, H.; Leal-Calderon, F.; Héroguez, V.; Schmitt, V. Pickering Emulsions: What Are the Main Parameters Determining the Emulsion Type and Interfacial Properties? *Langmuir* **2014**, *30*, 9313–9326.

(8) Liang, F.; Shen, K.; Qu, X.; Zhang, C.; Wang, Q.; Li, J.; Liu, J.; Yang, Z. Inorganic Janus Nanosheets. *Angew. Chem. Int. Ed.* **2011**, *50*, 2379–2382.

(9) Garbin, V.; Crocker, J. C.; Stebe, K. J. Nanoparticles at fluid interfaces: Exploiting capping ligands to control adsorption, stability and dynamics. *J. Colloid Interf. Sci.* **2012**, *387*, 1–11.

(10) Sashuk, V.; Hołyst, R.; Wojciechowski, T.; Fiałkowski, M. Close-packed monolayers of charged Janus-type nanoparticles at the air-water interface. *J. Colloid Interface Sci.* **2012**, *375*, 180 – 186.

(11) Fernandez-Rodriguez, M. A.; Rodriguez-Valverde, M. A.; Cabrerizo-Vilchez, M.; Hidalgo-Alvarez, R. Surface activity and collective behaviour of colloidally stable Janus-like particles at the air-water interface. *Soft Matter* **2014**, 3471–3476.

(12) Maestro, A.; Guzmán, E.; Ortega, F.; Rubio, R. G. Contact angle of micro- and nanoparticles at fluid interfaces. *Curr. Opin. Colloid Interface Sci.* **2014**, *19*, 355–367.

(13) Maestro, A.; Guzman, E.; Santini, E.; Ravera, F.; Liggieri, L.; Ortega, F.; Rubio, R. G. Wettability of silica nanoparticle-surfactant nanocomposite interfacial layers. *Soft Matter* **2012**, *8*, 837–843.

(14) Synytska, A.; Kirillova, M. S.; Isa, L. Synthesis and Contact Angle Measurements of Janus Particles. *ChemPlusChem* **2014**, *79*, 656–661.

(15) Jiang, S.; Chen, Q.; Tripathy, M.; Luijten, E.; Schweizer, K. S.; Granick, S. Janus Particle Synthesis and Assembly. *Adv. Mater.* **2010**, *22*, 1060–1071.

(16) Binks, B. P.; Fletcher, P. D. I. Particles Adsorbed at the Oil-Water Interface: A Theoretical Comparison between Spheres of Uniform Wettability and "Janus" Particles. *Langmuir* **2001**, *17*, 4708–4710.

(17) Yan, L.-T.; Xie, X.-M. Computational modeling and simulation of nanoparticle self-assembly in polymeric systems: Structures, properties and external field effects. *Progress in Polymer Science* **2013**, *38*, 369–405.

(18) Isa, L.; Lucas, F.; Wepf, R.; Reimhult, E. Measuring single-nanoparticle wetting properties by freeze-fracture shadow-casting cryo-scanning electron microscopy. *Nat. Commun.* **2011**, *2*.

(19) Stöber, W.; Fink, A.; Bohn, E. *J. Colloid Interface Sci.* **1970**, *33*, 67.

(20) Qiang, W.; Wang, Y.; He, P.; Xu, H.; Gu, H.; Shi, D. Synthesis of Asymmetric Inorganic/Polymer Nanocomposite Particles via Localized Substrate Surface Modification and Miniemulsion Polymerization. *Langmuir* **2008**, *24*, 606–608.

(21) Takahara, Y. K.; Ikeda, S.; Ishino, S.; Tachi, K.; Ikeue, K.; Sakata, T.; Hasegawa, T.; Mori, H.; Matsumura, M.; Ohtani, B. Asymmetrically Modified Silica Particles: A Simple Particulate Surfactant for Stabilization of Oil Droplets in Water. *J. Am. Chem. Soc.* **2005**, *127*, 6271–6275.

(22) Ge, X.; Wang, M.; Yuan, Q.; Wang, H.; Ge, X. The morphological control of anisotropic polystyrene/silica hybrid particles prepared by radiation miniemulsion polymerization. *Chem. Commun.* **2009**, 2765–2767.

(23) Fernandez-Rodriguez, M. A.; Song, Y.; Rodriguez-Valverde, M. A.; Chen, S.; Cabrerizo-Vilchez, M. A.; Hidalgo-Alvarez, R. Comparison of the Interfacial Activity between Homogeneous and Janus Gold Nanoparticles by Pendant Drop Tensiometry. *Langmuir* **2014**, *30*, 1799–1804.

(24) Montes Ruiz-Cabello, F.; Rodriguez-Valverde, M.; Cabrerizo-Vilchez, M. Contact angle hysteresis on polymer surfaces: an experimental study. *J. Adhes. Sci. Technol.* **2011**, *25*, 2039–2049.

(25) Liu, Z.; Guo, R.; Xu, G.; Huang, Z.; Yan, L.-T. Entropy-Mediated Mechanical Response of the Interfacial Nanoparticle Patterning. *Nano Letters* **2014**, *14*, 6910–6916.

(26) Fan, H.; Resasco, D. E.; Striolo, A. Amphiphilic Silica Nanoparticles at the Decane-Water Interface: Insights from Atomistic Simulations. *Langmuir* **2011**, *27*, 5264–5274.

(27) Stancik, E. J.; Kouhkan, M.; Fuller, G. G. Coalescence of Particle-Laden Fluid Interfaces. *Langmuir* **2004**, *20*, 90–94.

(28) Vogel, N.; Ally, J.; Bley, K.; Kappl, M.; Landfester, K.; Weiss, C. K. Direct visualization of the interfacial position of colloidal particles and their assemblies. *Nanoscale* **2014**, *6*, 6879–6885.

(29) Snoeyink, C.; Barman, S.; Christopher, G. F. Contact Angle Distribution of Particles at Fluid Interfaces. *Langmuir* **2015**, *31*, 891–897.

(30) Ma, Y.; Cao, X.; Feng, X.; Ma, Y.; Zou, H. Fabrication of super-hydrophobic film from PMMA with intrinsic water contact angle below 90°. *Polymer* **2007**, *48*, 7455–7460.

(31) Maestro, A.; Bonales, L. J.; Ritacco, H.; Rubio, R. G.; Ortega, F. Effect of the spreading solvent on the three-phase contact angle of microparticles attached at fluid interfaces. *Phys. Chem. Chem. Phys.* **2010**, *12*, 14115–14120.

(32) Xu, H.; Melle, S.; Golemanov, K.; Fuller, G. Shape and Buckling Transitions in Solid-Stabilized Drops. *Langmuir* **2005**, *21*, 10016–10020.

(33) Zang, D.; Stocco, A.; Langevin, D.; Wei, B.; Binks, B. P. An ellipsometry study of silica nanoparticle layers at the water surface. *Phys. Chem. Chem. Phys.* **2009**, *11*, 9522–9529.

(34) Kaz, D. M.; McGorty, R.; Mani, M.; Brenner, M. P.; Manoharan, V. N. Physical ageing of the contact line on colloidal particles at liquid interfaces. *Nat. Mater.* **2012**, *11*, 138–142.

(35) Walther, A.; Müller, A. H. E. Janus Particles: Synthesis, Self-Assembly, Physical Properties, and Applications. *Chem. Rev.* **2013**, *113*, 5194–5261.

(36) Iwashita, Y.; Kimura, Y. Orientational order of one-patch colloidal particles in two dimensions. *Soft Matter* **2014**, *10*, 7170–7181.

(37) Xu, H.; Kirkwood, J.; Lask, M.; Fuller, G. Charge Interaction between Particle-Laden Fluid Interfaces. *Langmuir* **2010**, *26*, 3160–3164.

(38) Kumar, A.; Park, B. J.; Tu, F.; Lee, D. Amphiphilic Janus particles at fluid interfaces. *Soft Matter* **2013**, *9*, 6604–6617.